Desalination and Water Treatment
www.deswater.com

doi:10.5004/dwt.2018.22962

131 (2018) 317–327
November

Iron ions reclaiming from sludge resulted from hot-dip galvanizing process, as Mg_3 Fe-layered double hydroxide used in the degradation process of organic dyes

Alin Golban, Laura Cocheci, Radu Lazau*, Lavinia Lupa, Rodica Pode*

Politehnica University Timisoara, Faculty of Industrial Chemistry and Environmental Engineering, 6 VasilePârvan Boulevard, 300223, Timisoara, Romania, Tel. +40256 404168, email: radu.lazau@upt.ro (R. Lazau), Tel. +40256403070, email: rodica.pode@upt.ro (R. Pode)

Received 20 March 2018; Accepted 12 August 2018

ABSTRACT

Iron sludge resulted from the neutralization of waste waters resulted during hot-dip galvanizing process was reclaimed in order to obtain a Fe(III) precursor solution used for the synthesis of Mg_3Fe-layered double hydroxide. The Fe(III) precursor solution was extracted from the sludge with three inorganic acids. The influence of the inorganic acid type, concentration, contact time and solid to liquid ratio upon the extraction efficiency of the iron ions was determined. Two types of Mg_3Fe-layered double hydroxides (LDH) were synthesized as follows: the first one was obtained starting from reagents and the second one from the iron precursor extracted from sludge. Both were characterized via X-ray powder diffraction (XRD), FT-IR spectroscopy, BET, TEM and SEM-EDX analysis. The results showed that the LDH obtained from the iron solution extracted from the recycled sludge had similar characteristics with the synthesized LDH from reagents. The photocatalytic activity of the both samples, in the degradation process of Congo Red, was also evaluated and was observed that the LDH obtained from sludge has photocatalytic properties almost similar to that synthetized from analytical grade reagents. All the results show the possibility of replacing the LDH synthesized from reagents with a viable, cheaper and green route of obtaining this material.

Keywords: Hot-dip galvanizing sludge; Extraction; Iron precursor; LDH synthesis; Photo catalysis; Congo Red degradation

1. Introduction

The 7th Environment Action Program of European Union sets out a long-term vision promoting "living well, within the limits of our planet" and foresees a Europe in 2050 in which "our prosperity stems from an innovative, *circular economy* where nothing is wasted and natural resources are managed sustainable" [1]. In the context of the Directive of wastes 2008/98/EC, which encourages the study of innovative reuse of wastes and the Framework Water Directive 2000/60/EC referring the progressive reduction of emissions of hazardous substances to water, the use of water treatment sludge as precursor of layered double hydroxides is a promising approach. Hot-dip galvanizing process is the most used process for the corrosion protection of steel. However, it is called a "dirty" process because of the high amount and variety of generated wastes [2–5]. In the hot-dip galvanizing process, the water resulted after washing, degreasing and pickling steps is neutralized and an iron-rich sludge is obtained. Until now, the recover and reuse of iron ions from such wastewater was not studied. Most of the studies regarding the heavy metals recovering are focused on the sewage sludge [7–10] or electroplating sludge, especially for chromium recovery [11–13]. The disposal of sludge, that is considered hazardous waste because ofits heavy metal content can cause water and soil pollution [5,14]. To prevent this type of pollution and, at the same time to recover the useful elements, it is necessary to remove the heavy metals using different treatment methods [14]. Three main processes are mentioned in the literature:

*Corresponding author.

pyrometallurgical, hydrometallurgical and solidification/stabilization method [3,4,14–19]. Pyrometallurgical treatments reduce the volume and the toxicity of the sludge; it could also reduce the leaching concentration of heavy metals. However, the main disadvantages of the pyrometallurgical processes are represented by the high energy use and the low final product purity [3,4,16]. The solidification/stabilization methods use materials such as cement in order to immobilize the heavy metals into solid matrixes. Yet, through these methods the volume of the potential toxic waste is increased due to the possible leaching in time of the heavy metals from the solid matrix [14]. Considering the hydration and leaching characteristics of the galvanic sludge and the economical, energy efficiency and environmental aspect of hydrometallurgical processes, these are usually preferred compared to the pyrometallurgical processes [15–19]. Chemical extraction of heavy metals demonstrated this is one of the most convenient approaches due to the simple operation, high removal efficiency and short extraction time. Moreover, the main advantage is represented by the possibility of the waste sludge reclaiming as secondary raw material, highly emphasizing resource reuse [7,10,12,19]. Several extracting chemicals were studied to obtain the highest possible level of recovery rates and selectivity for recovering of heavy metals from various sludge, such are: organic acids (acetic, citric or oxalic acid) [17–20], chelating agents (EDTA) [20], alkaline reagents and inorganic acids (HCl, HNO_3, H_2SO_4) [18–22]. Thus, the present paper studies the removal of iron (Fe) ions from industrial sludge originated from a hot-dip galvanizing plant in order to obtain precursors for synthesis of layered double hydroxides. Layered double hydroxides (LDH) are" anionic clays" with positively charged layers with two kinds of metallic cations and exchangeable hydrated gallery anions [23,24]. LDH have technological importance in catalysis, separation technology, optics, medical science and nanocomposite material engineering [25,26]. All the studies report the obtaining of the LDH starting from pure chemical reagents [23,25–28]. The aim of the present paper is to synthesize Mg_3Fe-LDH using as a precursor the iron ions recovered from the galvanic sludge. For the obtaining of the iron ions precursor, the chemical extraction process was studied. Three inorganic acids were used as extracting agents. The influence of extracting agent type, concentration and extraction time were investigated. Mg_3Fe-type layered double hydroxides were synthesized, one from reagents ($Mg(NO_3)_2{\cdot}6H_2O$ and $Fe(NO_3)_3{\cdot}9H_2O$) and the second one from $Mg(NO_3)_2{\cdot}6H_2O$ reagent and the iron precursor extracted from sludge. Both were characterized through X-ray powder diffraction (XRD), BET, SEM and EDX, TEM and FT-IR spectroscopy analysis. The obtained materials were used in the degradation process of Congo Red from aqueous solutions. The studies focused on the Congo Red degradation since the organic dyes are used in many industries and even a small amount released in the environment can affect the human health and the living organisms [29–31]. Therefore, the removal of dyes from waste waters is still a worldwide concern. Many studies have been done for the removal of toxic dyes from aqueous solutions through adsorption [30–33]. But it has been demonstrated that combining the sorption properties with the photocatalytic activity of different materials is more efficient in the removal process of dyes from aqueous solutions [34–37]. Therefore, the synthesized and characterized LDH were used as photocatalysts in the removal process of Congo Red from aqueous solutions.

2. Materials and methods

2.1. Sludge characterization

The sludge was collected from a hot-dip galvanizing plant located in Timisoara, Romania. It was dried at 105ºC to constant mass. Afterword the sludge was sieved and the majority fraction, between 90 and 160 μm, was used for further investigations. In order to determine the chemical composition of the sludge, it was mineralized with aqua reggia ($HCl:HNO_3 = 3:1$). The concentration of iron (Fe) was determined by volumetric method at pH = 2 with EDTA (0.05 M) using sulfosalicylic acid as titration indicator. The other metals were analyzed using a Varian SpectraAA 280 FS atomic adsorption spectrophotometer. The sludge was also subjected to phase analysis by X-ray diffraction, morphology by SEM-EDX and thermal analysis. The powder X-Ray diffraction patterns of the sludge were recorded at room temperature using a RigakuUltima IV instrument, with $Cu_{K\alpha}$ radiation (λ = 1.5418Å). SEM imaging was performed using a Quanta FEG 250 microscope, equipped with an EDAX/ZAF quantifier. The TG-DSC curves under non-isothermal conditions were recorded with a Netzsch STA 449 C instrument in static air atmosphere in the range of 25ºC ÷1000ºC, with a heating rate of 10ºC min^{-1}.

2.2. Obtaining of iron precursor

The extraction of iron ions was conducted under magnetic stirring at room temperature using three inorganic acids (HCl, HNO_3 and H_2SO_4) at various concentrations (10%, 15% and 20% each) and at various stirring time (15, 30, 45, 60, 75 and 90 min), using stoichiometric ratio between the iron sludge and acid solutions. The influence of the use in excess of the acid solutions (10, 15 and 20%) upon the extraction efficiency was also determined. In each case the phase separation was carried by centrifugation at 6000 rpm for 5 min.

2.3. Synthesis of Mg_3Fe-LDH

The synthesis method of Mg_3Fe-LDH consist in co-precipitation at low oversaturation, as described by Cavani et al. [23]. As trivalent cation (iron) precursor a calculated amount of solution was used, obtained from acid dissolution of sludge (LDH-S) or $Fe(NO_3)_3{\cdot}9H_2O$ analytical grade reagent for preparation of a blank sample (LDH-R). A measured amount of $Mg(NO_3){\cdot}6H_2O$ analytical grade reagent was also used for both samples, in order to obtain a molar ratio Mg/Fe = 3 and the total concentration of cations in 200 cm^3 solution of 1 M. This solution was added dropwise to a 1 M solution of Na_2CO_3, under vigorous magnetic stirring and keeping the pH value to 11.5 by means of 2 M NaOH solution. The brown-red precipitate was maintained under stirring for 2 h after the incorporation of cations solution was finished and then aged at 70°C for 18 h, washed several times with distilled water in order to remove the unre-

acted substances, filtered and dried at 70°C over night. The obtained samples were crushed to powders and sieved. The fractions lower than 90 μm were used in further analysis. Both of the synthesized samples were subjected to X-ray diffraction, BET, SEM-EDX, TEM and FTIR analysis. Surface areas, pore volumes and the adsorption-desorption isotherms of the as-synthesized and calcined samples were determined by N_2 adsorption-desorption at 77 K, using the BET analysis method, using a Micromeritics ASAP 2020 instrument. Before analysis the samples were degassed at 100°C for 72 h. The morphology of the samples was investigated using a FEI Tecnai F20 G2 TWIN TEM at an accelerating voltage of 200 kV in bright field mode. The powder was placed on a carbon film copper grid. The excess was removed by vigorous shaking. The UV-Vis diffuse reflectance spectrum of the LDH was obtained on a UV-VIS Carry 100 Varian spectrophotometer. The FTIR spectra (KBr pellets) were recorded on a Shimadzu Prestige- 21 FTIR spectrophotometer in the range 4000–400 cm^{-1}.

Since the present study is dealing with a real sample (a sludge resulted during hot-dip galvanizing process), in order to avoid errors caused by sample inhomogeneity, the entire results are presented as an average of three sets of experiments.

2.4. Evaluation of the photocatalytic activity of Mg_3Fe-LDH

The photocatalytic experiments were developed in a PhotoLAB B400-700 Basic Batch-L photoreactor provided by Peschl-Ultraviolet GmbH, which consists of a submerged 150 W Hg medium pressure lamp (TQ 150 type) that emits light in both ultraviolet and visible domain. 500 mg/L, 700 mL solution of Congo Red at its natural pH = 8.75, was mixed with 1 g/L catalyst (Mg_3Fe-R or Mg_3Fe-S) for 30 min in the dark in order to achieve the equilibrium, then the lamp was switched on. Samples were collected at defined time intervals, filtered throughout a Millipore syringe filter (45 μm pore size) and the UV-VIS spectra of Congo Red solutions were recorded by using a Varian Cary UV-VIS spectrophotometer. The concentration of the dye in the bulk solution at the end of the adsorption in the dark was considered as initial concentration value for the photocatalytic process.

3. Results and discussion

3.1. Sludge characterization

The experimental data regarding the chemical composition of the sludge are presented in Table 1. It can be observed that the sludge resulted from the neutralization of the waste solutions resulted from hot-dip galvanizing process has a high content of iron ions (34.4%). It also contains 8.95% of Ca (due to the fact that the neutralization of the waste solutions was carried using lime) and small amounts of impurities, such as: Pb, Cu and Mn.

The XRD pattern of the sludge resulted during hot-dip galvanizing process, presented in Fig. 1, shows that the studied material is mainly amorphous. The crystalline phases identified were: LepidocrociteFeO (OH) (DB card number: 10111088) – which represent the major component

Table 1
The chemical composition of sludge

Nr. Crt.	Species	Concentration, %
1.	Fe	34.4
2.	Ca	8.95
3.	Zn	1.62
4.	Mn	0.37
5.	Pb	1.19×10^{-2}
6.	Cu	2.70×10^{-2}

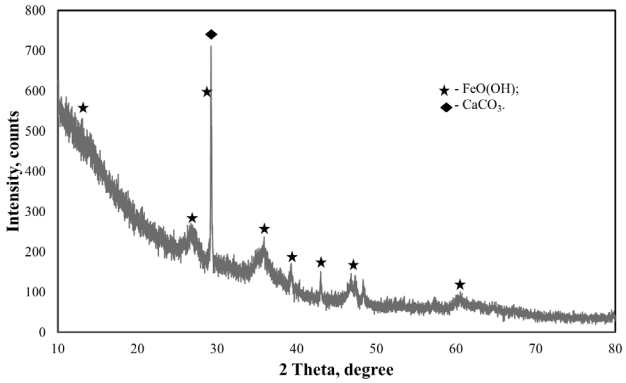

Fig. 1. XRD pattern of the iron sludge.

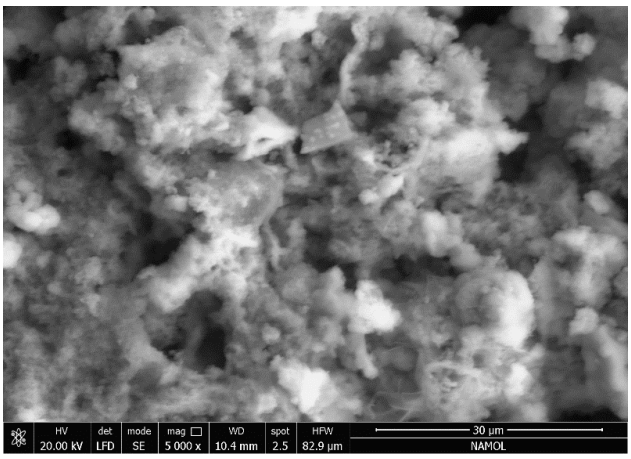

Fig. 2. SEM image of the iron sludge.

of the sludge, in accordance with the results obtained from the chemical analysis and calcite $CaCO_3$ (DB card number: 9009667). The presence of calcite is due to the neutralization agent used for the treatment of the waste solution resulted during hot-dip galvanizing process. The other impurities present in the sludge were not detected because of their content lower than 5%.

The morphology of the sludge was examined through SEM analysis and the image is presented in Fig. 2. It can be observed that the particles of the iron sludge are irregular, with large grain size distribution presenting some degree of agglomeration. This inhomogeneity of the samples can lead to the obtaining of irreproducible results in the extraction of

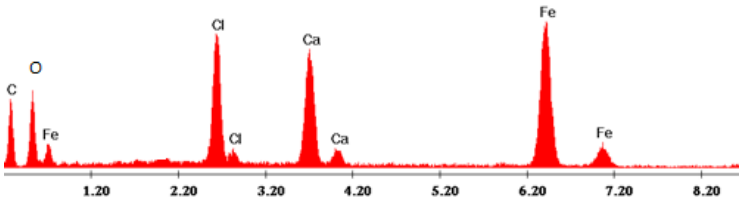

Elem.	Wt %
C	21.6
O	25.1
Cl	8.75
Fe	35.9
Ca	8.65
Total	100

Fig. 3. EDX spectrum of the iron sludge.

iron ions process. In order to avoid this drawback, the acid treatment was performed in triplicate and the results were presented as an average.

The EDX spectrum presented in Fig. 3 confirms the major component of the sludge is iron. The chlorine ions are present maybe from the acid used in the pickling step. Even if the EDX analysis is a semi-quantitative one, the results regarding the content of iron and calcium ions (the major components of the sludge) are in accordance with those obtained from the chemical analysis.

The DSC curve recorded on the iron sludge (Fig. 4) shows three endothermic peaks corresponding to three mass loss steps. The first step, with a weight loss of 15.33%, evolving with the maximum rate at 100.4°C, is due to the loss of humidity of the material. The second step with a weight loss of 5.93% and maximum rate at 260°C, corresponds to the dehydroxylation of iron oxy-hydroxide with formation of iron oxides. The third step with maximum rate at 642°C and a weight loss of 3.41% corresponds to the decarbonation of the material with calcium oxide formation.

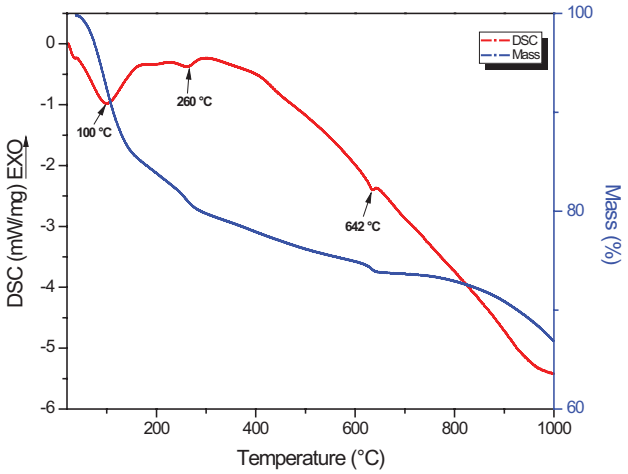

Fig. 4. TG-DSC curves recorded on the iron sludge.

3.2. Obtaining of iron precursor

The experimental data regarding the dependence of iron ions extraction efficiency function of the concentration of the used inorganic acids and function of stirring time are presented in Fig. 5.

It can be observed that for all the studied inorganic acids the extraction efficiency of iron ions increases with the increasing of the acid concentrations. H_2SO_4 has the highest extraction efficiency compared to HNO_3 and HCl. The extraction efficiency of Fe(III) depends on the stirring time. It improved when the contact time was increased from 15 to 60 min for all the studied acids. After 60 min of stirring, this influence is not so significant any longer.

Even if the extraction efficiency increases with the increase of the contact time, HCl and HNO_3 did not yield results as good as in the case of H_2SO_4 acid, when an extraction efficiency over 90% was achieved for 20% sulfuric acid solutions used as leaching media. Therefore, for the further experiments was used this solution as extraction agent.

The use of acid solution in excess leads to the linear increasing of the extraction process efficiency. The excess was not increased over 20% since for a solid: liquid ratio of S:L = 1:1.2 an extraction efficiency higher than 99% was achieved.

The solution of iron precursor which will be used in the synthesis process of LDH-S, obtained in the most efficient extraction conditions (use of H_2SO_4 20%, stirring time of 60 minutes and S:L ratio = 1:1.2), has the chemical composition presented in Table 2.

3.3. Characterization of the synthesized Mg_3Fe-LDH

The XRD patterns of the synthesized samples are presented in Fig. 7. As seen in Fig. 7, both XRD patterns reveal that a single phase is present in both materials: layered double hydroxide with well-ordered peaks, corresponding to the formula of pyroaurite: $Mg_6Fe_2CO_3(OH)_{16}{\cdot}4H_2O$ (DB card number 9009439). The basal peaks corresponding to (003) and (006) planes, characteristic for layered double hydroxides, are present at low 2θ values: 11.174° and 22.641° for LDH-R and 11.212° and 22.709° for LDH-S, respectively. The (110) and (113) reflections occurred at 2θ angles ranging from 59 to 61° and are also characteristic for layered double hydroxides. Both materials show good crystallinity. The calculated unit cell parameters and the crystallite size, together with the Mg/Fe ratios are presented in Table 3.

As seen in Table 3, the Mg/Fe ratio and the cell parameters in the synthesized materials have close values, but the average crystallite size of the particles is lower in the LDH-S. This could be assigned to the impurities of the iron precursor solution, which could induce a stress in the crystals growth. The metal content of the LDH-S was: 19.1% Mg; 15.2% Fe; $5.24 \cdot 10^{-2}$ % Zn; $7.44 \cdot 10^{-3}$% Mn; $1.32 \cdot 10^{-3}$% Cu; $1.28 \cdot 10^{-3}$% Pb. The Zn^{2+} ions, with the highest concentration among the impurities, could access the sites occupied by Mg^{2+} ions, but due to their ionic radius that are comparable with de six-folded Mg^{2+} ionic radius (r_{Mg2+} = 0.720 Å; r_{Zn2+} = 0.740 Å [37]), have not changed dramatically the unit cell parameters.

The N_2 adsorption-desorption isotherms and the pore size distribution of the two adsorbents are presented in Fig. 8.

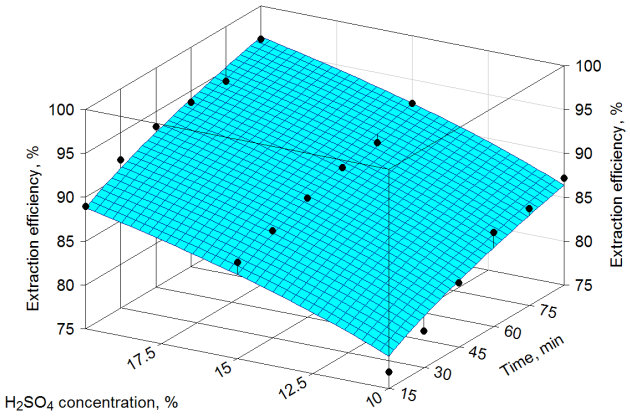

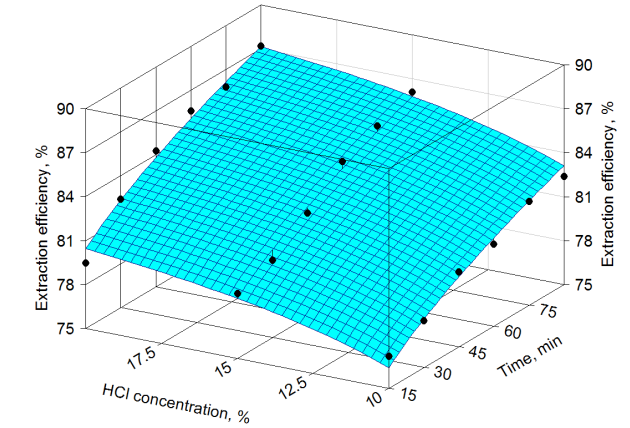

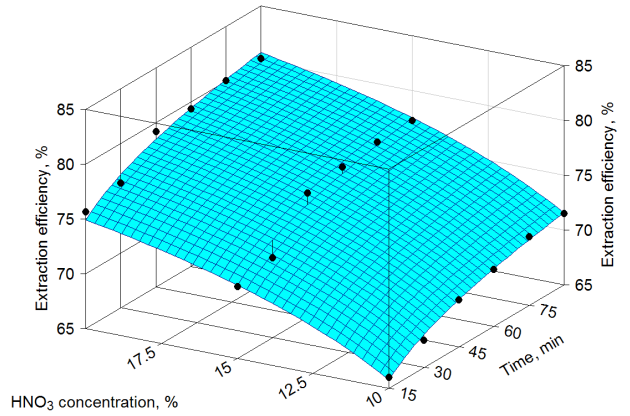

Fig. 5. The dependence of the Fe (III) extraction efficiency versus the acid concentration and contact time: a) H_2SO_4; b) HCl; c) HNO_3.

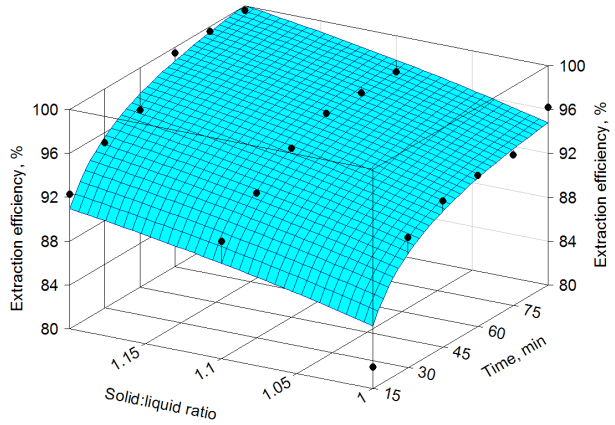

Fig. 6. The dependence of the Fe (III) extraction efficiency versus the S:L ratio.

Table 2
The chemical composition of the iron precursor solution

Nr. crt.	Species	Concentration, g/L
1.	Fe	84.0
2.	Zn	2.38
3.	Mn	5.81×10^{-1}
4.	Ca	2.84×10^{-1}
5.	Cu	6.64×10^{-2}
6.	Pb	$\times 10^{-2}$

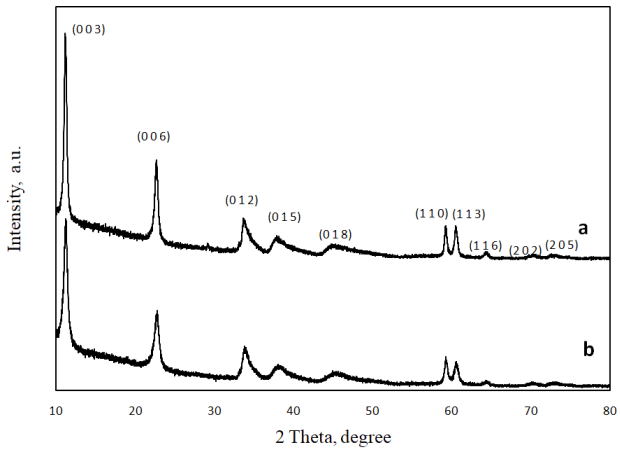

Fig. 7. XRD pattern of samples a) LDH-R and b) LDH-S.

The N_2 adsorption-desorption isotherms have the IV type shape, according to the IUPAC classification and H1-type hysteresis loops. The presence of the adsorption branches almost parallel with the desorption's ones shows the presence of tubular pores (mesopores type). In the pore distribution plot one can observe that the mesopores and macropores (40–100 nm) have the highest contribution to the textural properties of the studied materials.

The presence of impurities as sulfate ions in the structure of the obtained LDH-S is proved by the FTIR analysis. The FTIR spectra of the Mg_3Fe-LDH obtained from both iron precursors (sludge and reagent) are presented in Fig. 9.

It can be concluded that in both cases are obtained the same Mg_3Fe-LDH. In the IR spectra of both samples can be identified the following absorption bands: a very strong and broad band around 3462 cm^{-1} is assigned to the stretching vibration of H_2O molecules (ν_{O-H}) [23]; the broad shoulder at

Table 3
Unit cell parameters for the as-synthesized materials

Sample	Mg/Fe_t	Mg/Fe_p	a (Å)	c (Å)	c′ (Å)	D (Å)	S_{BET} (m^2/g)	V_p (cm^3/g)
LDH-R	3	2.98	3.120	23.75	7.917	111	50.8	0.504
LDH-S	3	2.87	3.118	23.67	7.890	76	73.4	0.560

Mg/Fe_t – the Mg/Fe ratio in the starting precursor solutions; Mg/Fe_p – the Mg/Fe ratio in the obtained materials; $a = 2 \cdot d_{(110)}$; $c = 3 \cdot d_{(003)} = 3 \cdot c'$, where c′ is the thickness corresponding to one brucite-like layer and one interlayer; the average crystallite size D was calculated by using Scherrer equation for the first three most intense peaks [28].

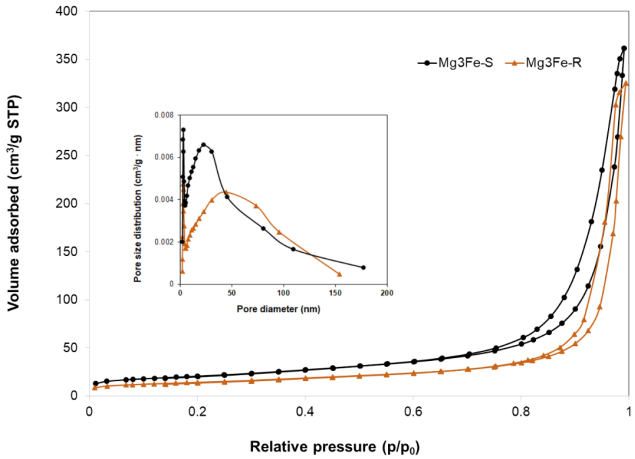

Fig. 8. N_2 adsorption-desorption isotherms and pore size distribution.

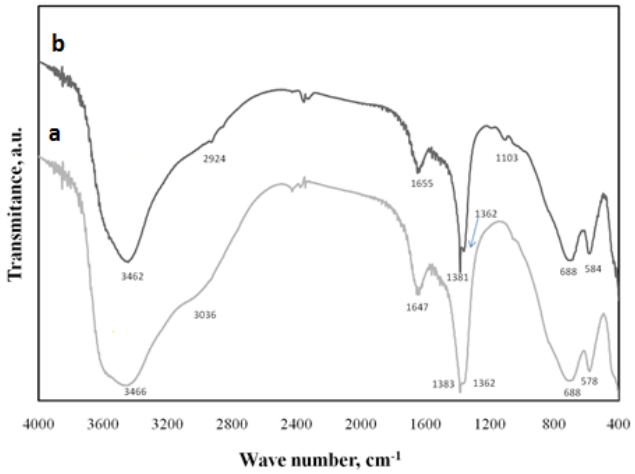

Fig. 9. FTIR spectra of a) LDH-R and b) LDH-S.

around 3000 cm^{-1} can be attributed to the hydrogen bonding between water and carbonate anion in the interlayer galleries; the weak band at around 1650 cm^{-1} was attributed to the bending vibration (δH_2O) of the H_2O molecules in the interlayer [24]; the bands at 1381 and 1362 cm^{-1} are characteristic to the CO_3^{2-} vibration [23]; the band at 689 cm^{-1} is attributed to $\nu_{M\text{-}O\text{-}M}$ vibration [24]; the band at 584 cm^{-1} is attributed to the metal–oxygen vibration [24]. Apart from this bands, the

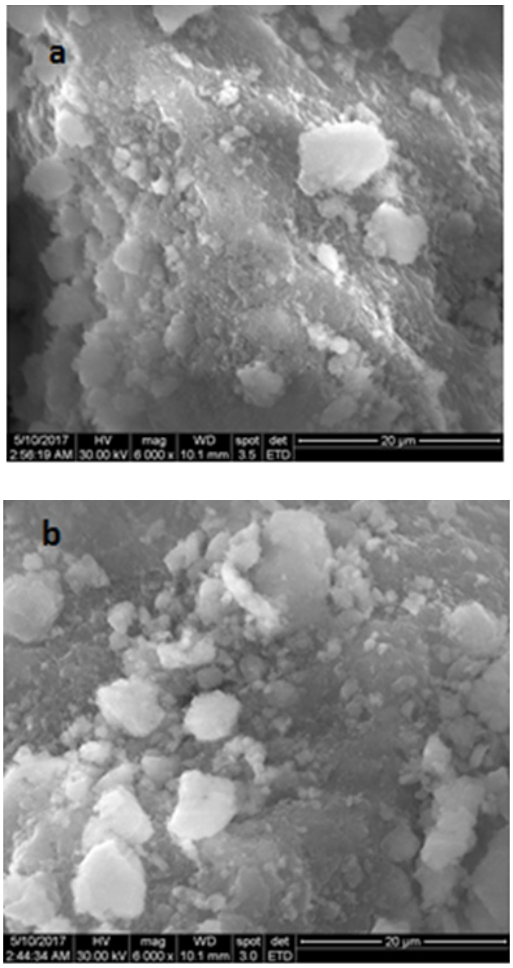

Fig. 10. SEM images of a) LDH-R and b) LDH-S.

sludge-obtained material presents a small intense band at 1103 cm^{-1}, which was attributed to the asymmetric bending vibrations of SO_4^{2-} [38], proving that a small amount of sulfate ions are present in the sludge-obtained LDH structure.

From the SEM images it can be seen that both Mg_3Fe-LDH obtained from reagents and also that obtained from iron reclaiming from sludge show similar morphology (Fig. 10) as fluffy particles. This type of crystal distribution is specific for the layered double hydroxides synthetized by co-precipitation method under low oversaturation. The elemental analysis and mapping were done using energy dispersive X-ray spectroscopy (EDX). The elemental mapping

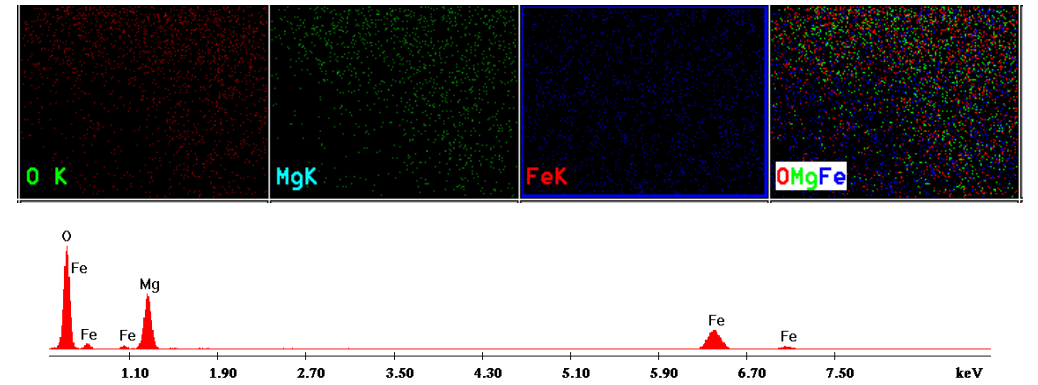

(a)

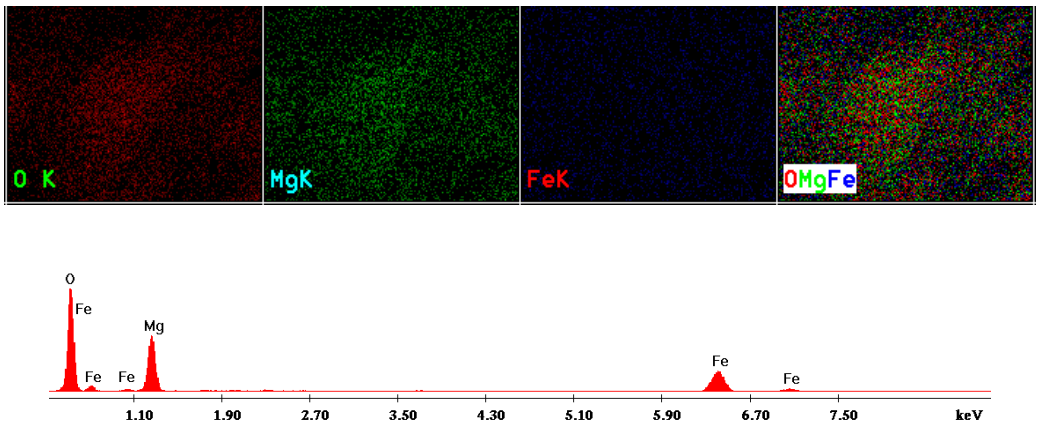

(b)

Fig. 11. EDX elemental mapping analysis of O, Mg and Fe of the a) LDH-R and b) LDH-S.

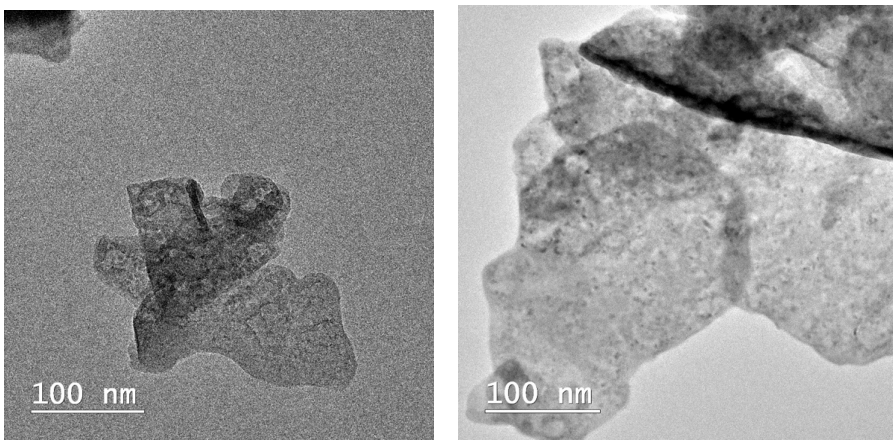

(a) (b)

Fig. 12. TEM image of a) LDH-R and b) LDH-S.

of the LDH are presented in Fig. 11, exhibiting a uniform distribution of Mg, Fe, and O in the synthesized samples.

The TEM micrograph showed that in both cases there were obtained well crystalized LDH and the hexagonal crystallites are arranged one above the other, both horizontally and vertically (Fig. 12).

The Kubelka-Munk transformed reflectance spectra are presented in Fig. 13. Were observed two band gap energies, due to the presence of LDH phase [39]. The first band gap (E_{g1}) is 4.81 eV for Mg_3Fe-S and 4.91 eV for Mg_3Fe-R. The second band gap (E_{g2}) for Mg_3Fe-S is 4.18 eV and 4.17 eV for Mg_3Fe-R. The obtained values are in agreement with

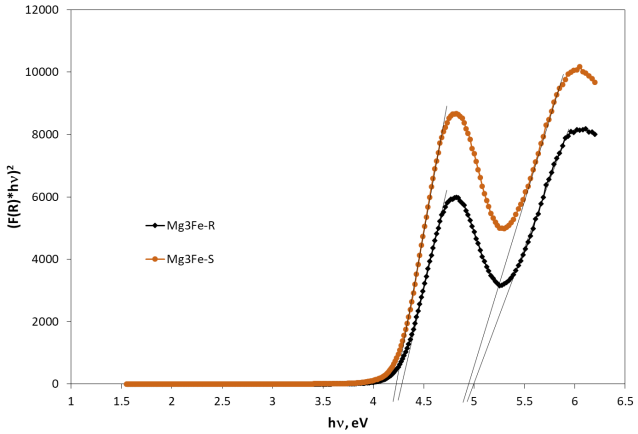

Fig. 13. Kubelka-Munk transformed reflectance spectra.

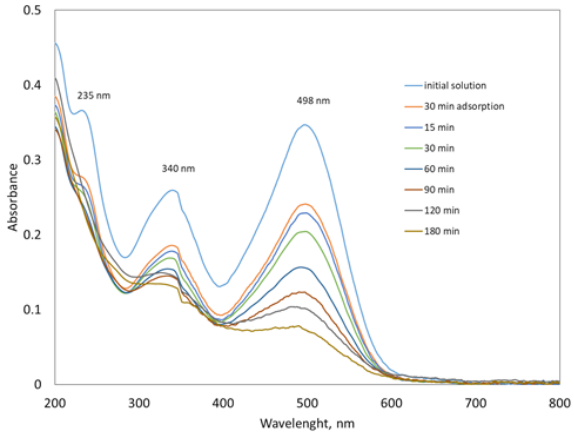

Fig. 14. The UV-VIS spectra of Congo Red solution recorded during the irradiation process by using Mg_3Fe-S as photocatalyst.

the literature, for diverse compositions of layered double hydroxides [39,40].

The entire analysis confirms the fact that the iron precursor solution obtained through extraction of iron ions from a secondary source can be efficiently used in the synthesis process of Mg_3Fe-LDH.

3.4. Photocatalytic activity of the synthesized Mg_3Fe-LDH

The UV-VIS spectra of Congo Red solution recorded during the irradiation process by using Mg_3Fe-S as photocatalyst are presented in Fig. 14. The solution of Congo Red exhibit a main absorption band in the visible region at 498 nm, assigned to the $\pi \rightarrow \pi^*$ transition in azo bond. The two absorption bands in the ultraviolet region appear at 340 and 235 nm and are attributable to the $\pi \rightarrow \pi^*$ transitions in naphthalene and benzene ring, respectively [41]. By observing changes in UV-VIS spectra within photocatalysis process for all three absorption bands, were obtained informations on dye discoloration and aromatic rings opening. While azo bonds are easy to break by UV irradiation, benzene and naphthalene rings opening are more difficult.

All three peaks became almost plat at the final time of irradiation, respectively at 180 mi, although the remaining absorbance intensity can be attributed to the organic intermediaries resulted during the photocatalytic process.

The effect of catalysts on Congo Red discoloration, compared with their performance as adsorbent materials is presented in Fig. 15. Without catalyst, only 0.2 of initial dye concentration is reduced, while in case of photocatalysts utilization, 0.8 of initial dye concentration is reduced. It can be observed that the equilibrium between the adsorbent and Congo Red is achieved in 30 min.

The discoloration efficiencies of the two catalysts are compared in Fig. 15. It could be observed that after 30 min of adsorption in the dark, the LDH prepared from sludge has 29.8% efficiency and the LDH prepared from analytical reagents has 23.1% efficiency on dye discoloration. This higher efficiency of the Mg_3Fe-S catalyst in the dye adsorption could be due to stress induced in the pyroaurite lattice by the presence of other cations as impurities (e.g. Zn^{2+}) from the precursor solution. Stress of crystalline lattice may

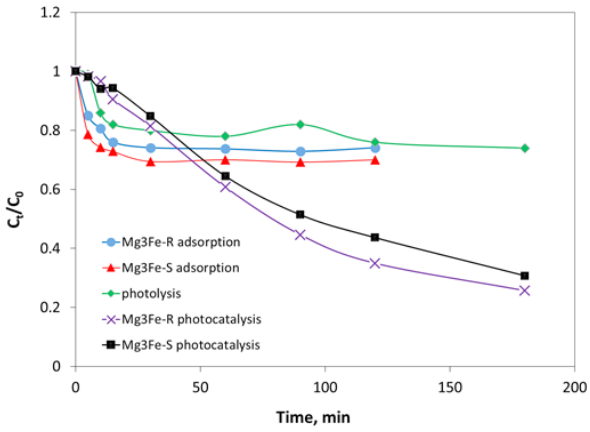

Fig. 15. Photolysis, adsorption and photocatalytic degradation of Congo Red using the studied materials.

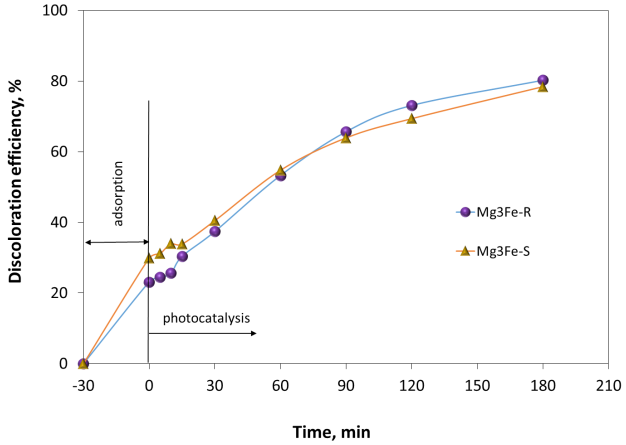

Fig. 16. The discoloration efficiency of the two photocatalysts.

result in a less crystallinity and in an increase in the number of adsorption sites [42]. After 180 min of irradiation, the efficiency of discoloration was 78.5% when Mg_3Fe-S was utilized as photocatalyst and 80.2% when Mg_3Fe-R was utilized as photocatalyst. The efficiency of Mg_3Fe-S material

was sensible smaller than those of Mg_3Fe-R material, probably due to its higher adsorption capacity. A greater amount of dye adsorbed on the surface of the material prevents UV radiation to activate the catalyst surface so that it generates less oxidant species [43]. In this way the photocatalysis is more difficult to carry out.

The dependencies of the dye discoloration, benzene and naphthalene rings opening rate on the irradiation time have been described by the Langmuir–Hinshelwood kinetic model [44] described by the equation:

$$r = \frac{dC}{dt} = \frac{kKC}{1+KC}$$

This equation can be simplified to a pseudo-first order equation:

$$\ln\left(\frac{C_t}{C_0}\right) = -kKt = -k_{app}t$$

where r is the rate of dye discoloration, naphthalene ring opening and benzene ring opening (mg/L/min), C_0 is the initial dye concentration (mg/L), C_t is the concentration of the dye at time t (mg/L), t is the irradiation time (min), k is the reaction rate constant (min^{-1}) and k_{app} is the apparent rate constant (min^{-1}).

The apparent rate constant for dye discoloration, naphthalene ring opening and benzene ring opening, k_{app}, was calculated from the intercept of the plot of $\ln(C_t/C_0)$ against time, t, for both materials utilized as photocatalysts (Figs. 17 and 18).

The kinetics results are presented in Table 4. For both utilized photocatalysts, the discoloration process occurred the fastest, and the benzene ring opening process was the slowest. The discoloration process and the naphthalene ring opening process of Congo Red occurs faster in the case of Mg_3Fe-R utilized as a photocatalyst, probably because the material has a lower adsorption capacity. In this case, UV radiation can more easily access the catalyst surface to initiate the oxidation process. The benzene ring opening apparent rate constant is greater in case of utilization Mg_3Fe-S as photocatalyst than in case of Mg_3Fe-R, showing that the process is faster probably due to the impurities present in the catalyst structure. These impurities (e.g. Zn^{2+}) could plays the role of additional catalysts for the benzene ring opening process.

The possible mechanism of photocatalytic degradation reaction of Congo Red is described below:

$Mg_3Fe\text{-}LDH + h\nu \rightarrow Mg_3Fe\text{-}LDH\ (e^-_{cb} + h^+_{vb})$

Congo Red + $Mg_3Fe\text{-}LDH\ (h^+_{vb}) \rightarrow$ Oxidation

$Mg_3Fe\text{-}LDH\ (h^+_{vb}) + H_2O \rightarrow Mg_3Fe\text{-}LDH + H^+ + OH^\bullet$

$Mg_3Fe\text{-}LDH\ (e^-_{cb}) + OH^- \rightarrow Mg_3Fe\text{-}LDH +$

Congo Red + $Mg_3Fe\text{-}LDH\ (e^-_{cb}) \rightarrow$ Reduction

$Mg_3Fe\text{-}LDH\ (e^-_{cb}) + O_2 \rightarrow Mg_3Fe\text{-}LDH + O_2^{\bullet-}$

$O_2^{\bullet-} + H^+ \rightarrow HO_2^\bullet$

$HO_2^\bullet + HO_2^\bullet \rightarrow H_2O_2 + O_2$

$H_2O_2 + O_2^{\bullet-} \rightarrow OH^\bullet + OH^- + O_2$

Congo Red + $OH^\bullet \rightarrow$ Degradation products

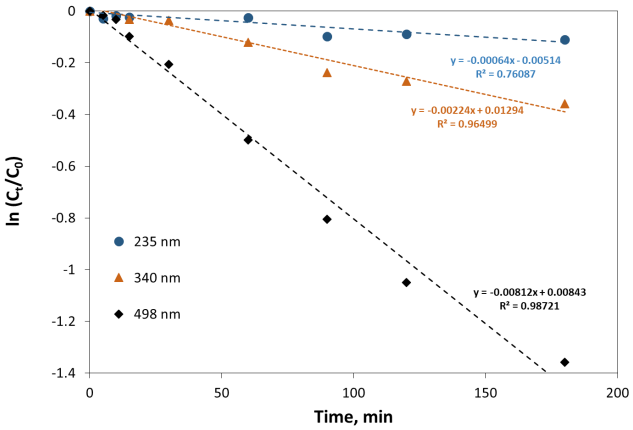

Fig. 17. Pseudo-first order kinetic model for Congo Red degradation by using Mg_3Fe-R as photocatalyst.

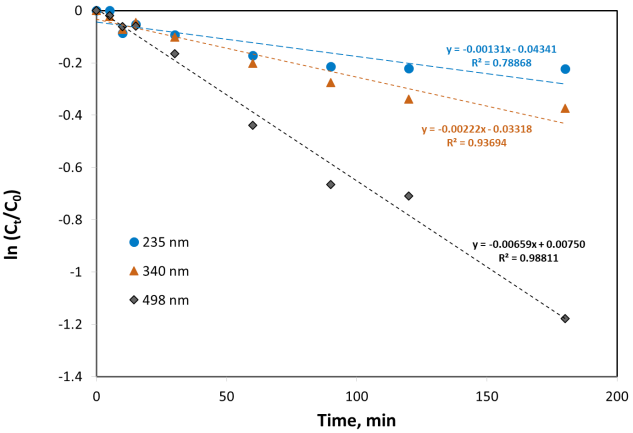

Fig. 18. Pseudo-first order kinetic model for Congo Red degradation by using Mg_3Fe-S as photocatalyst.

In conclusion, the LDH obtained from sludge has photocatalytic properties almost similar to that synthetized from analytical grade reagents. Based on the entire analysis the following scheme was proposed for iron ions reclaiming from sludge resulted during the neutralization of waste waters discharged from hot dip galvanizing industry (Fig. 19). To obtain 1 kg of Mg_3Fe-LDH it is necessary to use 2.2 kg of iron sludge resulted from hot dip galvanizing process and 0.67 kg concentrated H_2SO_4 solution.

The proposed technology of Mg_3Fe-LDH obtaining, using as iron precursor an iron solution reclaimed from the sludge resulted during hot dip galvanizing process, presents the following advantages: (1) the quantity of waste sludge discharged in the environment is reduced; (2) the costs of waste management of the hot dip galvanizing industry are reduced; (3) valuable elements from an industrial sludge are recovered and capitalized; (4) the consumption of prime material for the LDH synthesis is reduced; (5) the overall cost of LDH obtaining process is reduced; (6) it is a process that can be easily implemented at industrial scale. All these proves the viability of this cheaper, green route of obtaining this material. The obtained Mg_3Fe – LDH can successfully

Table 4
Apparent rate constants for dye discoloration and aromatic rings opening

	Discoloration, 498 nm		Naphthalene ring opening, 340 nm		Benzene ring opening, 235 nm	
	k_{app} (min^{-1})	R^2	k_{app} (min^{-1})	R^2	k_{app} (min^{-1})	R^2
Mg_3Fe-R	8.12×10^{-3}	0.98721	2.24×10^{-3}	0.96499	0.64×10^{-3}	0.76087
Mg_3Fe-S	6.59×10^{-3}	0.98811	2.22×10^{-3}	0.93694	1.31×10^{-3}	0.78868

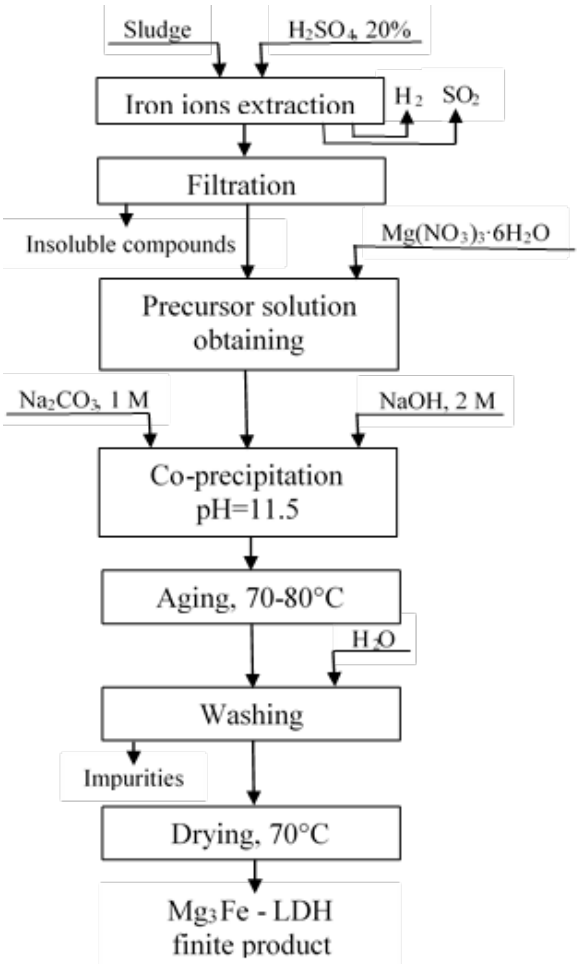

Fig. 19. The technological scheme of iron ions reclaiming from sludge resulted from hot-dip galvanizing process, as Mg_3Fe - layered double hydroxide.

be used as photcatalyst materials in the treatment process of water with dye content.

4. Conclusion

The iron ions from sludge resulted during hot-dip galvanizing process were reclaimed as Mg_3Fe-LDH. The Fe(III) precursor solution was obtained with highest efficiency under extraction of iron ions from the sludge with 20% sulfuric acid solution, using a stirring time of 60 min and a S:L ratio = 1:1.2. The similarities of Mg_3Fe-LDH obtained, by co-precipitation method under low oversaturation, using the iron precursor from a secondary source and Mg_3Fe-LDH obtained using pure reagents were identified by the RX, FTIR, TEM and SEM analysis. The entire analysis confirms the fact that the iron precursor solution obtained through extraction of iron ions from hot-dip galvanizing sludge can be efficiently used in the synthesis process of layered double hydroxides. Furthermore, the obtained Mg_3Fe-LDH obtained from secondary sources presented also a very good efficiency as photocatalyst in the degradation process of Congo Red from aqueous solutions. Through this new proposed route of Mg_3Fe-LDH obtaining, using as iron precursor an iron solution reclaimed from the sludge resulted during hot dip galvanizing process is reduced the amount of sludge discharged in the environment and is diminished the use of pure reagents for LDH synthesis, leading to the significantly cost saving.

Acknowledgments

This work was supported by a grant of the Romanian National Authority for Scientific Research and Innovation, CNCS - UEFISCDI, project number PN-II-RU-TE-2014-4-0771. The studies were done during the PhD program from the Doctoral School of the University Politehnica Timisoara.

References

[1] Decision No 1386/2013/EU of the European Parliament and of the Council of 20 November 2013 on a General Union Environment Action Programme to 2020 'Living well, within the limits of our planet', Official Journal of the European Union, L354, 56, 2013, 171–200.
[2] C. Stocks, J. Wood, S. Guy, Minimisation and recycling of spent acid wastes from galvanizing plants, Resour. Conserv. Recy. 444 (2005) 153–166.
[3] M.D. Turan, H.S. Altundoğan, F. Tümen, Recovery of zinc and lead from zinc plant residue, Hydrometallurgy, 75 (2005) 169–176.
[4] G. Rossini, A.M. Bernardes, Galvanic sludge metals recovery by pyrometallurgical and hydrometallurgical treatment, J. Hazard. Mater., 131 (2006) 210–216.
[5] L. Lupa, P. Negrea, A. Iovi, M. Ciopec, M. Motoc, Zinc oxide obtaining from zinc ash, Rev. Chim. (Bucharest, Rom.), 58 (2007) 1075–1079. [In Romanian]
[6] L. Lupa, A. Iovi, P. Negrea, A. Negrea, G. Szabo, Recovery of zinc and iron from the sludge resulted during thermal zinc coating, Environ. Eng. Manag. J., 5 (2006) 1099–1112.
[7] M.A. Stylianou, D. Kollia, K.-J. Haralambous, V.J. Inglezakis, K.G. Moustakas, M.D. Loizidou, Effect of acid treatment on the removal of heavy metals from sewage sludge, Desalination, 215 (2007) 73–81.
[8] N.C. Shiba, F. Ntuli, Extraction and precipitation of phosphorus from sewage sludge, Waste Manage., 60 (2016) 191–200.

[9] X. Wang, J. Chen, X. Yan, X. Wang, J. Zhang, J. Huang, J. Zhao, Heavy metal chemical extraction from industrial and municipal mixed sludge by ultrasound-assisted citric acid, J. Ind. Eng. Chem., 27 (2015) 368–372.
[10] J. Deng, X. Feng, X. Qiu, Extraction of heavy metal from sewage sludge using ultrasound-assisted nitric acid, Chem. Eng. J., 152 (2009) 177–182.
[11] P.T. de Souza e Silva, N.T. de Mello, M.M.M. Duarte, M.C.B.S.M. Montenegro, A.N. Araújo, B. de Barros Neto, V.L. da Silva, Extraction and recovery of chromium from electroplating sludge, J. Hazard. Mater., 128 (2006) 39–43.
[12] C. Li, F. Xie, Y. Ma, T. Cai, H. Li, Z. Huang, G. Yuan, Multiple heavy metals extraction and recovery from hazardous electroplating sludge waste via ultrasonically enhanced two-stage acid leaching, J. Hazard. Mater., 178 (2010) 823-833.
[13] R. Su, B. Liang, J. Guan, Leaching effects of metal from electroplating sludge under phosphate participation in hydrochloric acid medium, Procedia Environ. Sci., 31 (2010) 361–365.
[14] F. Andreola, L. Barbieri, F. Bondioli, M. Cannio, A.M. Ferrari, I. Lancelloti, Synthesis of chromium containing pigments from chromium galvanic sludges, J. Hazard. Mater., 156 (2008) 466–471.
[15] Y.-C. Kuan, I.-H.Lee, J.-M. Chern, Heavy metal extraction from PCB wastewater treatment sludge by sulfuric acid, J. Hazard. Mater., 177 (2010) 881–886.
[16] F.A.D. Amaral, V.S. dos Santos, A.M. Bernardes, Metals recovery from galvanic sludge by sulfate roasting and thiosulfate leaching, Miner. Eng., 60 (2014) 1–7.
[17] J.D. Chou, C.L. Lin, M.Y. Wey, S.H. Chang, Effect of Cu species on leaching behavior of simulated copper sludge after thermal treatment: ESCA analysis, J. Hazard. Mater., 179 (2010) 1106–1110.
[18] J.E. Silva, A.P. Paiva, D. Soares, A. Labrincha, F. Castro, Solvent extraction applied to the recovery of heavy metals from galvanic sludge, J. Hazard. Mater., 120 (2005) 113–118.
[19] T. Kinoshita, K. Yamaguchi, S. Akita, S. Nii, F. Kawaizumi, K. Takahashi, Hydrometallurgical recovery of zinc from ashes of automobile tire wastes, Chemosphere, 59 (2005) 1105–1111.
[20] M. Gheju, R. Pode, F. Manea, Comparative heavy metal chemical extraction from anaerobically digested biosolids, Hydrometallurgy, 108 (2011) 115–121.
[21] S.M. Shin, G. Senanayake, J.-S. Sohn, J.-G. Kang, D.-H. Yang, T.-H. Kim, Separation of zinc from spent zinc-carbon batteries by selective leaching with sodium hydroxide, Hydrometallurgy, 96 (2009) 349–353.
[22] F. Xie, T. Cai, Y. Ma, H. Li, C. Li, Recovery of Cu and Fe from Printed Circuit Board waste sludge by ultrasound: Evaluation of industrial application, J. Clean. Prod., 17 (2009) 1494–1498.
[23] F. Cavani, F. Trifirò, A. Vaccari, Hydrotalcite-type anionic clays: Preparation, properties and applications, Catal. Today, 11 (1991) 173–301.
[24] L. Cocheci, P. Barvinschi, R. Pode, E. Popovici, E.M. Seftel, Structural characterization of some Mg/Zn-Al type hydrotalcites prepared for chromate sorption from wastewater, Chem. Bull. "Politehnica" Univ. (Timisoara), 55(1) (2010) 40–45.
[25] J.Q. Jiang, S.M. Ashekuzaman, Preparation and evaluation of layered doublehydroxides (LDHs) for phosphate removal, Desal. Water. Treat., 55 (2015) 836–843.
[26] O.P. Ferreira, O.L. Alves, D.X. Gouveia, A.G. Souza Filho, J.A.C. de Paiva, J.M. Filho, Thermal decomposition and structural reconstruction effect on Mg–Fe-based hydrotalcite compounds, J. Solid State Chem., 177 (2004) 3058–3069.
[27] J. Liu, X. Yue, Y. Yu, Y. Guo, Adsorption of sulfate from natural water on calcined Mg–Fe layered double hydroxides, Desal. Water. Treat., 56 (2015) 274–283.
[28] K.B. Rozov, U. Berner, D.A. Kulik, L.W. Diamond, Solubility and thermodynamic properties of carbonate-bearing hydrotalcite-pyroaurite solid solutions with a 3:1 Mg/(Al+Fe) mole ratio, Clay. Clay Miner., 59 (2011) 215–232.
[29] P. Kumar, R. Agnihotri, K.L. Wasewar, H. Uslu, C.K. Yoo, Status of adsorptive removal of dye from textile industry effluent, Desal. Water. Treat., 50 (2012) 226–244.
[30] Mu. Naushad, Z.A. Alothman, Md.R. Awual, S.M. Alfadul, T. Ahamad, Adsorption of rose Bengal dye from aqueous solution by amberlite Ira-938 resin: kinetics, isotherms, and thermodynamic studies, Desal. Water. Treat., 57 (2016) 13527–13533.
[31] S.M. Twang, M.A.A. Zaini, L.Md. Salleh, M.A.C. Yunus, Mu. Naushad, Potassium hydroxide-treated palm kernel shell sorbents for the efficient removal of methyl violet dyed, Desal. Water. Treat., 84 (2017) 262–270.
[32] A.B. Albadarin, M.N. Collins, Mu. Naushad, S. Shirazian, G. Walker, C. Mangwandi, Activated lignin-chitosan extruded blends for efficient adsorption of methylene blue, Chem. Eng. J., 307 (2017) 264–272.
[33] A.A. Alqadami, Mu. Naushad, M.A. Abdalla, M.R. Khan, Z.A. Alothman, Adsorptive removal of toxic dye using Fe_3O_4-TSC nanocomposite: Equilibrium, kinetic and thermodynamic studies, J. Chem. Eng. Data, 61 (2016) 3806–3813.
[34] D. Pathania, G. Sharma, A. Kumar, Mu. Naushad, S. Kalia, A. Sharma, Z.A. Alothman, Combined sorptional-photocatalytic remediation of dyes by polyaniline Zr(IV) selenotungstophosphate nanocomposite, Toxicol. Environ. Chem., 97 (2015) 526–537.
[35] D. Pathania, D. Gupta, A.H. Al-Muhtaseb, G. Sharma, A. Kumar, Mu. Naushad, T. Ahamad, S.M. Alshehri, Photocatalytic degradation of highly toxic dyes using chitosan-g-poly (acrylamide)/ZnS in presence of solar irradiation, J. Photochem. Photobio. A: Chem., 329 (2016) 61–68.
[36] A. Kumar, G. Sharma, Mu. Naushad, P. Singh, S. Kalia, Polyacrylamide/$Ni_{0.02}Zn_{0.98}O$ nanocomposite with high solar light photocatalytic activity and efficient adsorption capacity for toxic dye removal, Ind. Eng. Chem. Res., 53 (2014) 15549–15560.
[37] R.D. Shannon, Revised effective ionic radii and systematic study of inter atomic distances in halides and chalcogenides, ActaCrystallogr., A32 (1976) 751–767.
[38] A. Fahami, G.W. Beall, Mechanosynthesis and characterization of hydrotalcite like Mg–Al–SO_4-LDH, Mater. Lett., 165 (2016) 192–195.
[39] S. Babakhani, Z.A. Talib, M.Z. Hussein, A.A.A. Ahmed, Optical and thermal properties of Zn/Al-layered double hydroxide nanocomposite intercalated with sodium dodecyl sulfate, J. Spectrosc. (2014) http://dx.doi.org/10.1155/2014/467064.
[40] N. Ahmed, Y. Shibata, T. Taniguchi, Y. Izumi, Photocatalytic conversion of carbon dioxide into methanol using zinc–copper–M(III) (M = aluminum, gallium) layered double hydroxides, J. Catal., 279 (2011) 123–135.
[41] R. Jiang, J. Yao, H. Zhu, Y. Fu, Y. Chang, L. Xiao, G. Zeng, Effective decolorization of congo red in aqueous solution by adsorption and photocatalysis using novel magnetic alginate/γ-Fe_2O_3/CdS nanocomposite, Desal. Water. Treat., 52 (2014) 238–247.
[42] N. Chubar, R. Gilmour, V. Gerda, M. Micusik, M. Omatsova, K. Heister, P. Man, J. Fraissard, V. Zaitsev, Layered double hydroxides as the next generation inorganic anion exchangers: Synthetic methods versus applicability, Adv. Colloid. Interf.e Sci., 245 (2017) 62–80.
[43] K.M. Reza, A.S.W. Kurny, F. Gulshan, Parameters affecting the photocatalytic degradation of dyes using TiO_2: a review, Appl. Water Sci., 7 (2017) 1569–1578.
[44] M. Dinari, M.M. Momeni, Y. Ghayeb, Photodegradation of organic dye by ZnCrLa-layered double hydroxide as visible-light photocatalysts, J. Mater. Sci.: Mater. Electron., 27 (2016) 9861–9869.